JOURNAL OF CATALYSIS 75, 7–22 (1982)

Methane Production from the Catalyzed Reaction of Graphite and Water Vapor at Low Temperatures (500–600 K)

A.L. CABRERA, HEINZ HEINEMANN, AND G. A. SOMORJAI

Materials and Molecular Research Division, Lawrence Berkeley Laboratory, and Department of Chemistry, University of California, Berkeley, California 94720

Received September 3, 1981; revised December 1, 1981

The steady-state production of methane from the catalyzed reaction of high-density graphite and water vapor at low temperatures (500–600 K) is reported. The reaction is catalyzed by potassium hydroxide and potassium carbonate placed on the graphite surface. The steady-state production of methane has a turnover frequency of 10^{-3} sec^{-1} at 522 K and an activation energy of 10 ± 3 kcal/mole. Several other alkali hydroxides, lithium, sodium, and cesium hydroxide, all turned out to be good catalysts for the production of methane from water vapor and graphite. The surface composition and surface texture were characterized by Auger electron spectroscopy and scanning electron microscopy, respectively.

INTRODUCTION

The production of low-molecular-weight gaseous hydrocarbons directly from carbon or from various carbonaceous deposits (coal, unburned particulates, biomass) provides an intriguing alternative to liquefaction with hydrogen or to gasification to carbon monoxide and hydrogen at high temperatures (>1000 K). The reaction of carbon with water to produce methane and carbon dioxide,

$$2C + 2H_2O \rightarrow CH_4 + CO_2 \qquad (1)$$

is virtually thermoneutral $\Delta G_{600\,K} = +3$(kcal/mole) and thermodynamically feasible at low temperatures. Nevertheless, much of the research carried out to convert carbon to hydrocarbon liquids has concentrated on high-pressure reactions with hydrogen. Studies of coal gasification with water proved that high-temperature regimes were needed for efficient production of CO and H_2 (*1*). While recent studies by Exxon researchers (*2*) reported the production of substantial amounts of CH_4 along with CO and H_2 during coal gasification using K_2CO_3 as a catalyst, these studies have still employed relatively high temperatures (>900 K) which facilitate the decomposition of most hydrocarbons that would be produced.

Our research is focused on finding suitable catalysts for low-temperature production of low-molecular-weight hydrocarbon molecules from carbon (coal). We report the efficient conversion of high-density graphite to methane and CO_2 using potassium compounds as catalysts in the temperature range of 500 to 600 K. The reaction has a turnover frequency of 10^{-3} sec^{-1} at 522 K. While most of our studies have been carried out using clean graphite samples of ~1 cm^2, scale-up to produce large concentrations of methane appears feasible by using graphite powder with a much larger area. The potassium-catalyzed methane production was studied over samples of high-density graphite. The samples were either covered with potassium that was evaporated from an external source, *in situ*, in ultrahigh vacuum (UHV) or by impregnation with KOH or K_2CO_3, obtained from their respective solutions, prior to introducing the samples into the UHV chamber. In all three cases the steady-state rates of production of CH_4 were the same. Potassium also catalyzes the water–gas shift reaction:

$$CO + H_2O \rightarrow CO_2 + H_2 \qquad (2)$$

0021-9517/82/050007-16$02.00/0

in the temperature range 300–600 K; the K_2CO_3 covered graphite catalyzed this reaction (2) better than KOH-covered graphite. Potassium, however, did not catalyze the methanation reaction [$CO + 3H_2 \rightarrow CH_4 + H_2O$] under our experimental conditions and in this range of temperature.

Several other alkali hydroxides were also utilized as catalysts to compare their activity for the methane production with that of potassium hydroxide. Lithium hydroxide (LiOH) yielded the highest rate of CH_4 production; the cesium hydroxide (CsOH) activity was comparable to that of potassium hydroxide and sodium hydroxide (NaOH) was the least active catalyst.

EXPERIMENTAL

Several samples of graphite were cleaved in air with a razor blade from a larger piece of highly oriented pyrolytic graphite (HOPG) obtained from Union Carbide Corporation. The high-density material contained no hydrogen or oxygen. The samples were cut to a rectangular shape having geometric areas ranging from 0.65 to 1.00 cm^2 and a thickness of ~1 mm. The graphite sample was then mounted on the manipulator of a UHV system operating at a base pressure $<10^{-9}$ Torr. The graphite is held from both ends by gold wires.

When the sample holder was positioned properly inside the system, the sample surface was accessible to surface composition analysis by Auger electron spectroscopy (AES), ion sputter cleaning, and mass spectrometry. AES was performed with a cylindrical mirror analyzer from Physical Electronics Industries, Inc. that was mounted on movable bellows. The system was also equipped with a high-pressure cell which isolates the sample and allows us to perform chemical reaction studies at high pressures (up to 100 atm) without removing the sample from the UHV chamber. The product distribution obtained at high pressures were monitored by an HP 5880A gas chromatograph with a thermal conductivity detector and a 6-ft column of Chromosorb 102 in series with a 6-ft column of Chromosorb 101. This chromatographic column combination resolves H_2, CO, CH_4, and CO_2 at room temperature and H_2O when the gas chromatograph oven is heated to 150°C after the CO_2 peak has evolved. The thermal conductivity detector was sensitive enough to detect very small quantities of CO, CO_2, and CH_4. In the case of these gases, concentrations of one part per million (1 ppm) which correspond to 5×10^{14} molecules could be detected.

The graphite samples were heated resistively by a high-current AC power supply and the sample temperature monitored with a chromel-alumel thermocouple inserted between the graphite and one of the gold leads. This system is an improved version of a high-pressure–low-pressure instrument reported earlier (*3*). A schematic diagram of the system with the high-pressure cell closed or open is shown in Fig. 1.

Half a monolayer of potassium was deposited onto the graphite using a potassium-zeolite gun at a background pressure of 1×10^{-9} Torr. This potassium source consisted of a platinum filament coated with a potassium-alumino-silicate emitter and a collimator, similar to that described by Marbrow and Lambert (*4*). The potassium coverage of the sample was determined by monitoring the growth of the potassium layer on a piece of gold foil as a function of time by means of AES. Plotting the potassium Auger peak intensity at 252 eV as a function of deposition time, a layer-by-layer growth mechanism (*5*) was obtained. Once the time of deposition to form a half monolayer was determined, potassium was evaporated onto the graphite using identical experimental conditions. After the half monolayer of potassium was deposited onto the graphite, the high-pressure cell was closed and the sample was exposed to a mixture of water vapor and helium. This mixture consisted of 30 Torr of vapor obtained from distilled water and 1 atm of high-purity helium that was further purified by using a liquid nitrogen trap. The potassium-covered graphite

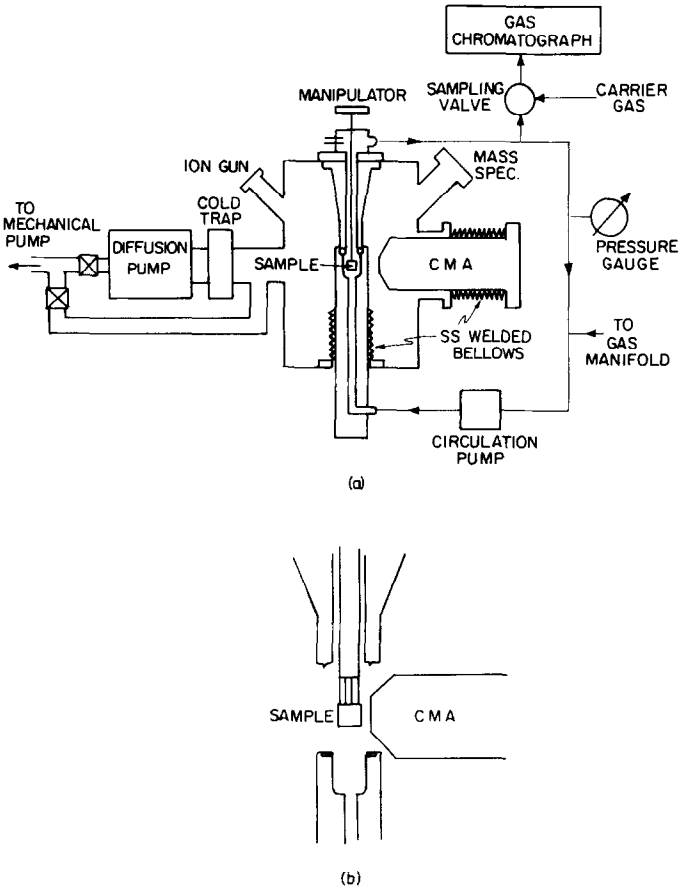

FIG. 1. (a) Schematic diagram of the apparatus with high-pressure cell closed, (b) detail with high-pressure cell open.

was then heated to the desired temperature in this gas mixture and the gas composition was analyzed every 10 min with the gas chromatograph for 4 to 24 hr. The cleanliness of the graphite surface and the potassium surface concentration was monitored by AES before and after the high-pressure experiments.

In another case, a solution of KOH with a molarity of 0.38 *M* was prepared, and the fresh sample of graphite already mounted on the manipulator was dipped into the solution and then dried in air. The KOH-covered graphite sample was then exposed to high vacuum for AES analysis. Once the cleanliness of the surface was checked, the isolation cell was closed and the sample was exposed to the water–helium gas mixture and heated to the desired temperature. The products' concentrations were measured with the gas chromatograph and the reaction was carried out under the same conditions used with the potassium-covered graphite samples. The sample surface was analyzed by AES before and after the experiments. This procedure was repeated at different reaction temperatures, each time using a fresh sample of graphite. When samples of graphite were coated with other alkali hydroxides (LiOH, NaOH, CsOH) or with K_2CO_3, solutions of these bases were made with the same molarity (0.38 *M*) as in the case of KOH, and the same procedure was used.

Thermal desorption experiments were performed using an EAI mass spectrometer

for the detection of the different desorption products. The mass spectrometer ionizer was placed at 5 cm from one of the sample faces; a nearly constant heating rate of 10 K/sec was employed in the range 300–1200 K to desorb the adsorbates.

A quartz microreactor technique (*6*) was employed to measure methane production from graphite powder impregnated with KOH. The purpose of these studies was to prove that the catalyzed production of CH_4 from graphite and water vapor could be readily scaled up to produce large quantities of CH_4.

In our apparatus, a mixture of helium and water was flowed over the sample which was placed in a temperature-controlled reactor. The exit of the reactor was attached to the sampling valve of the gas chromatograph and the gas flow vented to the atmosphere. Water vapor-saturated helium was obtained by bubbling a stream of helium through a closed container filled with distilled water. The partial pressure of water was ~40 Torr and the total pressure inside the rector was ~1 atm. The reactor consisted of a 6-mm-o.d. × 4-mm-i.d. × 30-cm-long quartz tube in a tube furnace, the temperature of which could be regulated to within ±5 K. The powdered graphite with KOH was held in the reactor tube with glass wool plugs. A chromel-alumel thermocouple enclosed in a thin walled 3-mm-o.d. quartz tube was inserted in one side of the reactor tube, making direct contact with the sample to monitor its temperature. This system is described in more detail elsewhere (*7*).

RESULTS AND DISCUSSION

K–Graphite System. (Half a Monolayer of Potassium Deposited on Graphite)

No chemical reaction between graphite and water vapor is detectable in the absence of the potassium catalyst. In the presence of potassium the production of CH_4 can be readily observed when this system is heated to 473 K. The concentration of CH_4, CO_2, and CO produced during the reaction of water vapor with the graphite samples were monitored as a function of time in the temperature range of 475–600 K. Hydrogen was detected among the reaction products, but due to the similarity of its thermal conductivity to that of the carrier gas (He), it was difficult to quantitatively follow its concentration change. The buildup of CH_4 concentration at two temperatures, 475 and 523 K, is displayed in Fig. 2. There is an initial high rate of methane production that, after about an hour, settles to a somewhat slower steady-state rate that can be maintained for extended periods of time in the temperature range 473–523 K. From this figure and similar data obtained at other temperatures, an activation energy for the production of CH_4 of 10 ± 3 kcal/mole can be estimated. A turnover frequency for the methane formation can be calculated assuming that all the graphite surface atoms are active sites. The steady-state rate of methane production obtained from Fig. 2 is divided by the number of surface atoms of the graphite sample. This number of surface atoms is estimated by assuming the presence of 1×10^{15} sites per 1 cm^2 of graphite (*8*). Once the number of sites was calculated from the geometric surface area of the graphite sample, a turnover frequency of $\sim 10^{-3}$ sec^{-1} at 523 K was obtained. Turnover frequencies for methane production catalyzed by various alkali hydoxides are listed in Table 1.

The concentration of CO_2 and CO that accumulated in the reaction chamber were about 10 and 30 times higher, respectively, than the CH_4 concentration. In order to determine whether there were other sources than graphite for the formation of the detected reaction products in the high-pressure chamber, several blank experiments were performed. A gold foil with and without potassium was substituted for the high-density graphite sample in the chamber and the experiments were repeated using identical conditions of water vapor pressures and temperature. No methane could be detected in this case. However, production of

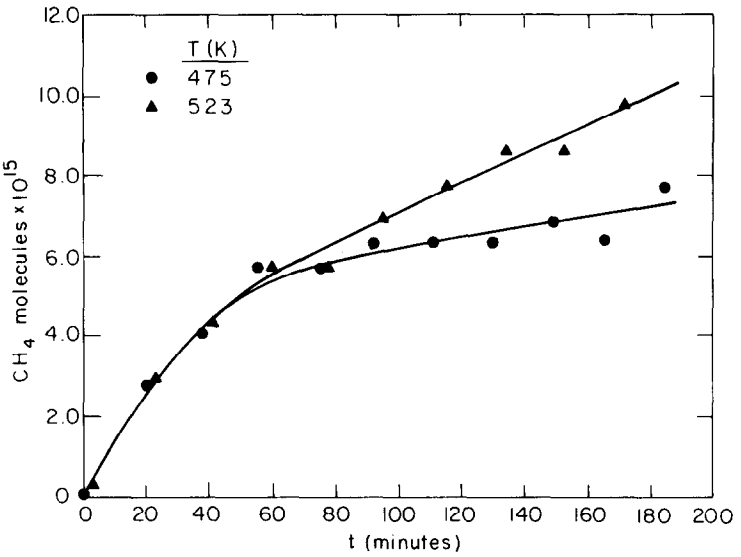

FIG. 2. Number of CH_4 molecules produced during the potassium-catalyzed water–graphite reaction as a function of time for two different temperatures.

CO_2 and CO could be observed at rates which are not too different from those detected in the presence of graphite. It appears that the walls of the stainless-steel reaction chamber provide a source of carbon for carbon oxide formation in the presence of water vapor. In order to obtain carbon mass balance for the graphite–water reaction that produces methane, the amounts of CO_2 and CO produced by the blank experiments must be subtracted from the total amount of CO_2 and CO detected under reaction conditions. The relative buildup of CO and CO_2 concentrations obtained with either the gold foil or with the graphite samples for the two temperatures (475 and 523 K) is displayed in Figs. 3 and 4, respectively. In the case of CO production, the concentration appears to be independent of temperature, and after subtracting the amount produced in the blank experiment there is no CO left within experimental error. However, the CO_2 concentration does depend on temperature and, after subtraction of the amount produced in the blank experiments, some CO_2 still remained, as seen in Fig. 4. It should be noted that in any UHV apparatus the residual gases which constitute the background of the system are H_2, H_2O, and CO, while methane and CO_2 are rarely present. Therefore, the uncertainty in the CO concentrations measured was much higher than those of CH_4 and CO_2. In the cases of CH_4 and CO_2, we could measure concentration variations of $\sim 5 \times 10^{14}$ and $\sim 3 \times 10^{15}$ molecules, respectively, but in the case of CO the uncertainty was $\pm 4 \times 10^{16}$ molecules.

Since the amount of CO_2 left after subtraction from the blank experiment is equiv-

TABLE 1

Methane Reaction Rates of the Water–Graphite Reaction Catalyzed by Various Alkali Hydroxides

System	Geometric surface area of graphite sample (cm^2)	Rate of CH_4[a] production (molecule/carbon surface atom × sec) ($\times 10^{-4}$)
LiOH–graphite	0.77	23.8
NaOH–graphite	0.81	5.6
KOH–graphite	0.72	9.9
CsOH–graphite	0.65	10.0

[a] It was assumed 1×10^{15} sites per 1 cm^2 of graphite.

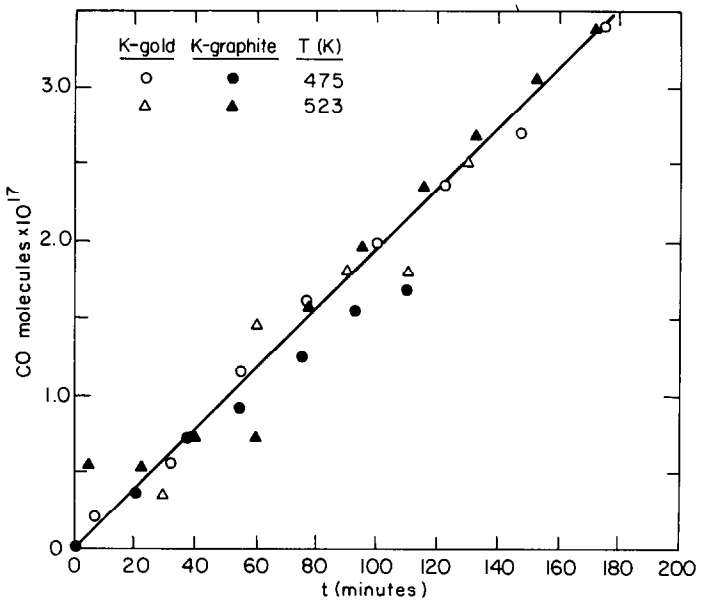

FIG. 3. Number of CO molecules produced as a function of time for two different temperatures. Open circles and triangles correspond to blank experiments performed with potassium-covered gold foils. Full circles and triangles correspond to experiments with potassium-covered graphite in the reaction chamber.

alent to the CH_4 concentration produced at the same temperature, we can write the reaction by which CH_4 is produced as: $2H_2O + 2C\ (\text{graphite}) \xrightarrow{K} CH_4 + CO_2$ (at 473–673 K).

The graphite–water reaction was studied

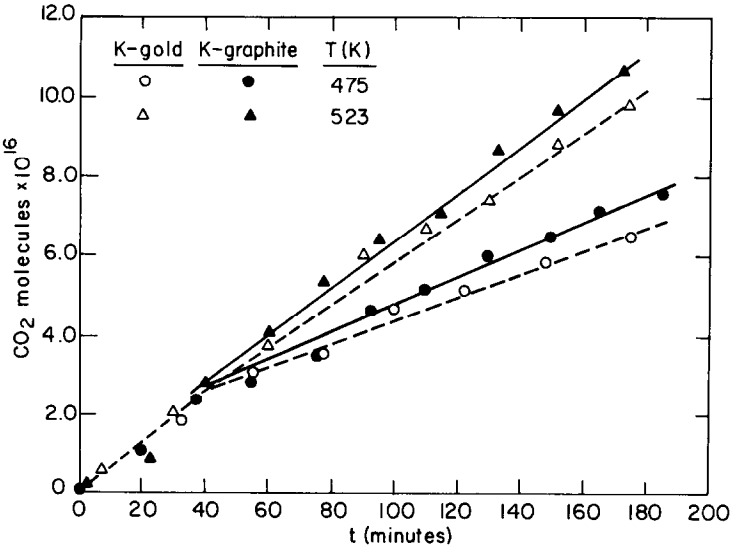

FIG. 4. Number of CO_2 molecules produced as a function of reaction time for two different temperatures. Dashed curves correspond to blank experiments performed with potassium-covered gold foil. Solid lines correspond to experiments with potassium-covered graphite in the reaction chamber.

in the temperature range of 473–673 K, and it was found that the highest conversion to CH_4 occurs at 523 K. Up to this temperature the rate of CH_4 production occurs in a steady state and there is no sign of catalyst poisoning. At temperature above 523 K, the potassium Auger peak diminishes with time and the surface is covered with an increasing concentration of carbonaceous species as detected by AES; simultaneously, the production of CH_4 slows down and then stops. After completion of a run, potassium was not readily detectable by AES.

When we exposed the K-covered graphite to a mixture of 1 atm of CO with 30 Torr of water vapor, H_2 and CO_2 formation could be detected. This indicates that the water–gas shift reaction was taking place but no CH_4 formation was observed. Methane was not detected when K-covered graphite was exposed to 1 atm of pure H_2 and the CH_4 production was not enhanced when H_2 was added to the water vapor with H_2 pressures of 20–700 Torr. It appears that CH_4 could not be formed from a mixture of CO and H_2 under our experimental conditions. In the presence of a gas mixture of 1 atm of CO_2 and 30 Torr of water vapor, no products of any kind were detected.

The KOH–Graphite System

The production of CH_4 was studied using graphite samples that were dipped in 0.38

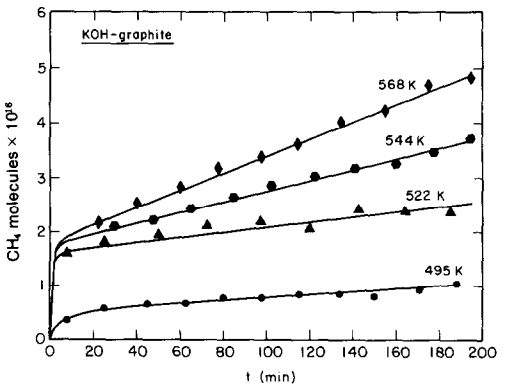

FIG. 5. Number of CH_4 molecules produced during the KOH-catalyzed water–graphite reaction as a function of reaction time for various temperatures.

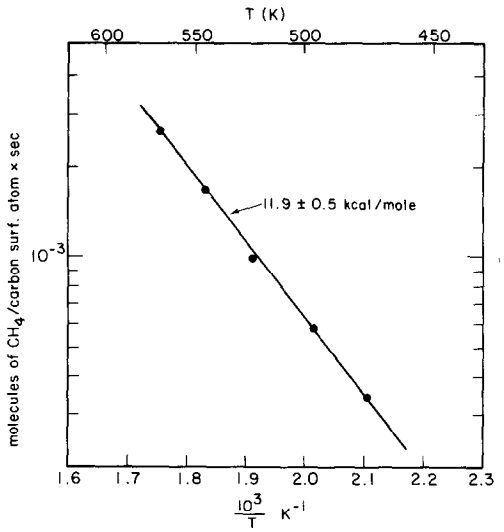

FIG. 6. Logarithm of the CH_4 production rate as a function of the inverse absolute temperature for the KOH–graphite system.

M KOH solution and then air-dried. The water vapor pressure in the H_2O/He mixture was the same as used previously, and our experiments were carried out in the temperature range 475–568 K. The accumulation of CH_4 as a function of time at various temperatures is displayed in Fig. 5. These curves exhibit larger initial rates of CH_4 production than those measured for the K–graphite system which appears in the first 5 min after the sample is heated to the preset temperature. Nevertheless, in steady state (after the initial burst) the methane production rates are identical. A plot of the logarithm of the steady state rates obtained from Fig. 5 divided by the number of carbon atoms of the graphite sample as a function of the inverse absolute temperature is shown in Fig. 6. From this plot an activation energy for the CH_4 production of 11.9 ± 0.5 kcal/mole is obtained. This activation energy is in good agreement with the 10 ± 3 kcal/mole that was estimated for the CH_4 production using the K–graphite system.

The CO and CO_2 concentrations were also monitored in this case. Most of the CO present in the gas phase is again CO desorbed from the high-pressure cell walls

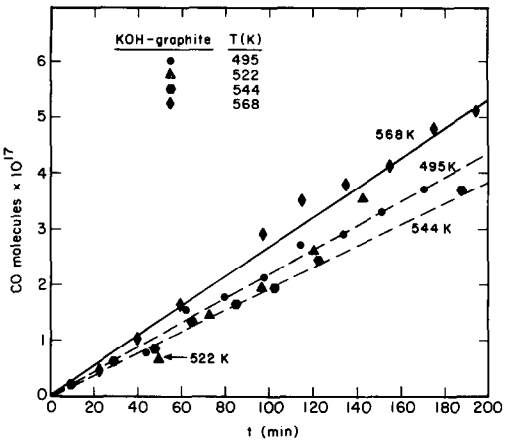

FIG. 7. Number of CO molecules produced during the KOH-catalyzed water–graphite reaction as a function of reaction time for various temperature.

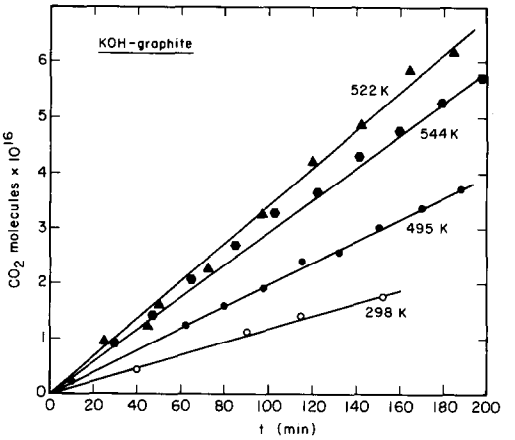

FIG. 8. Number of CO_2 molecules produced during the KOH-catalyzed water–graphite reaction as a function of reaction time for various temperatures. Open circles correspond to the production of CO_2 from the KOH-catalyzed water–gas shift reaction which takes place at room temperature.

and in the presence of water it readiiy reacts to form H_2 and CO_2 by means of the water–gas shift reaction [Eq. (2)]. The water–gas shift reaction achieves its maximum rate in the CO_2 and H_2 production at ~525 K and then at higher temperatures slows down and stops completely at ~568 K. The CO and CO_2 concentrations measured are displayed in Figs. 7 and 8, respectively. In Fig. 8 we have also plotted the CO_2 produced by the water–gas shift reaction which occurs at room temperature, 298 K (detectable CH_4 production starts up only at 475 K). No CO_2 is produced at 568 K. On the other hand, the CO concentration (Fig. 7) which remained almost independent of temperature and similar to that detected on a gold foil, covered with potassium, clearly is increased at 568 K, when CO_2 is no longer produced, indicating that the water–gas shift reaction is inhibited. This suggests that at these high temperatures the KOH catalyzed water vapor–graphite reaction produces primarily gaseous CH_4 and CO.

$$2H_2O + 3C\ (\text{graphite}) \xrightarrow[568\ K]{KOH} CH_4 + 2CO \quad (3)$$

Even though Eq. (3) is not thermoneutral at low temperature, it becomes thermodynamically more favorable at high temperatures ($\Delta G_{400\,K}$ = 26 kcal/mole; $\Delta G_{600\,K}$ = 14 kcal/mole).

In order to show more clearly the selectivities of the various reactions of water vapor over the KOH–graphite system, we have plotted the rate of CH_4, CO_2, and CO produced under our reaction conditions as a function of temperature in Fig. 9. In this figure the CO_2 production rate corresponds to the total concentration of CO_2 detected.

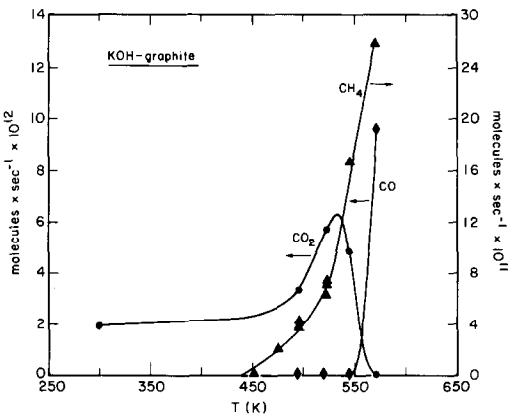

FIG. 9. Plot of the rates of CH_4, CO_2, and CO production during the KOH-catalyzed water–graphite reaction as a function of absolute temperature.

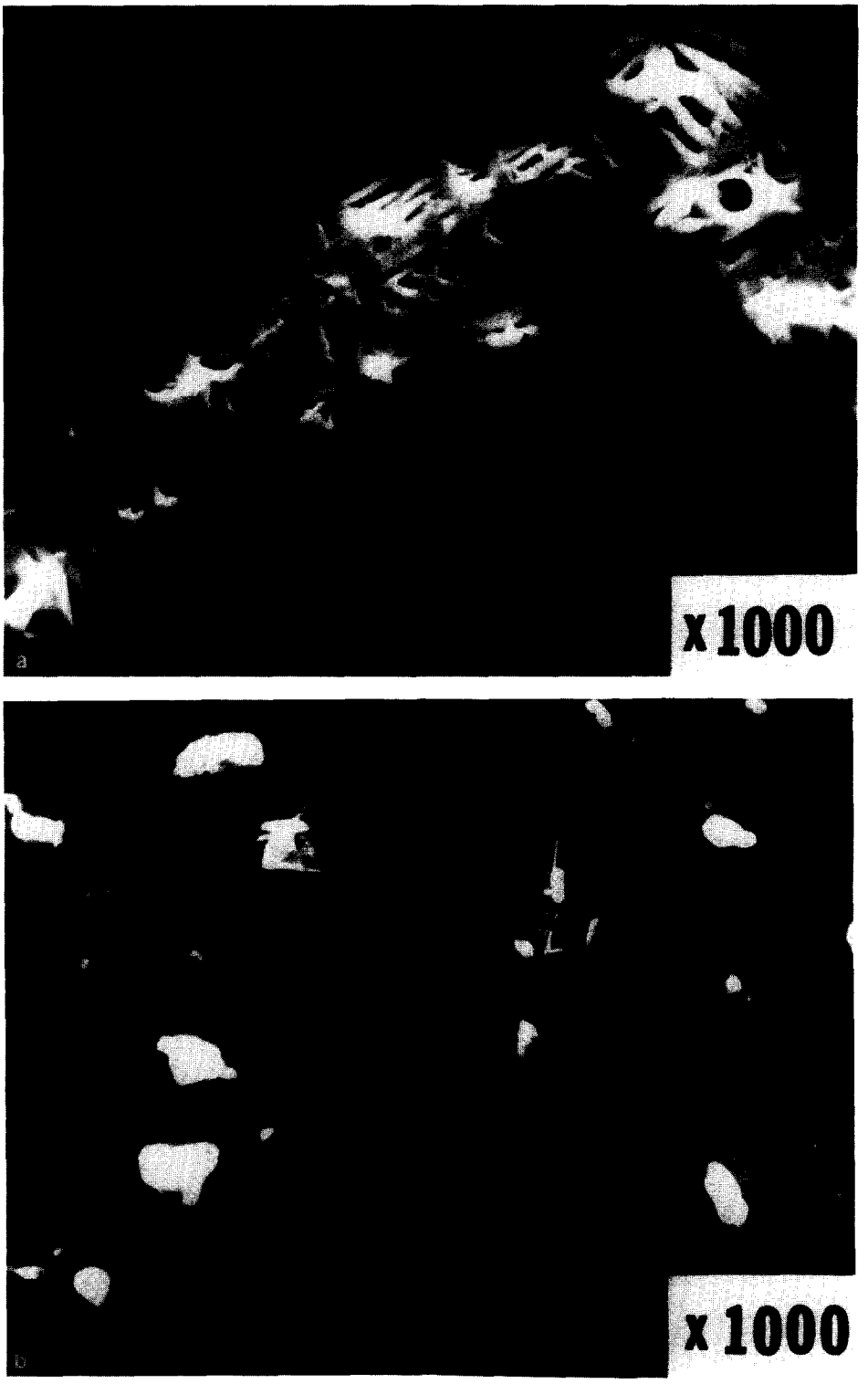

FIG. 10. SEM micrographs of KOH on graphite (a) before exposure to reaction conditions, (b) after exposure to reaction conditions.

The CO_2 produced along with the CH_4 according to Eq. (1) was very difficult to estimate because the CO_2 produced in the water–gas shift reaction (almost 90% of the total CO_2) was very sensitive to the KOH concentration on the surface of the graphite or on the gold foil used in blank experiments. Surface composition analysis by AES indicated a reduction in the intensity of the potassium peak (252 eV) after the sample was exposed to reaction conditions.

In order to learn about the structure of the active graphite surface and about the state of dispersion of KOH, samples of graphite coated with KOH were inspected by a scanning electron microscope (SEM) before and after being exposed to reaction conditions. Initially, the KOH crystallites cover the surface of the graphite fairly uniformly forming a weblike network as seen in Fig. 10a. After it is exposed to the reaction conditions, KOH agglomerates forming crystallites of a few microns in diameter, scattered over the graphite surface, as indicated in Fig. 10b. Thus the KOH–graphite contact area is markedly reduced. One can also notice in Fig. 10b roughened patches

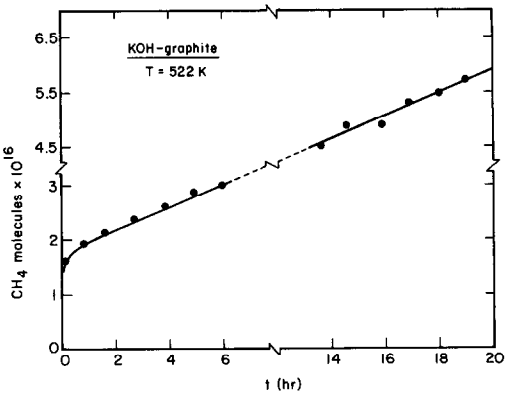

FIG. 11. Number of CH_4 molecules produced during the KOH-catalyzed water–graphite reaction as a function of reaction time, measured at 522 K for 20 hr.

that were absent before the water–graphite reaction. These patches are perhaps the locations where graphite was chemically attacked and produced CH_4.

The reduction in the contact surface between KOH and graphite is likely to be responsible at least in part for the reduced CH_4 rate of production after an initial period and for the steady-state rate being appreciably lower than the initial reaction rate.

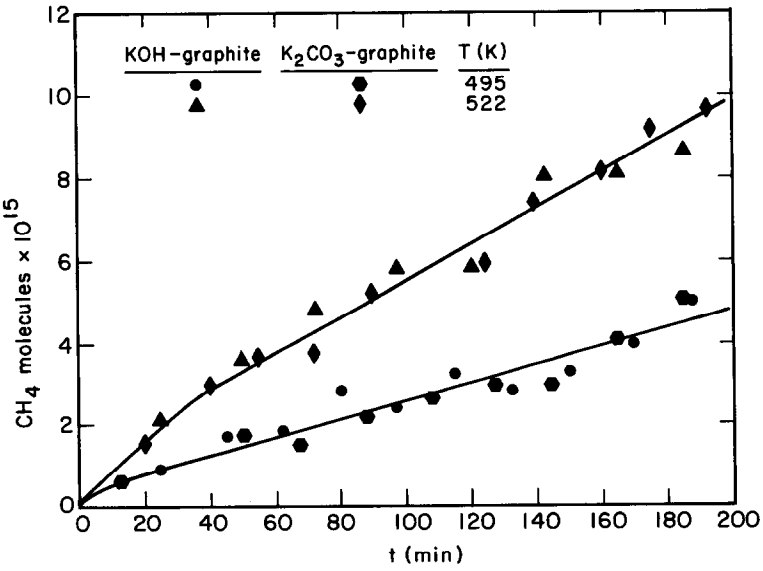

FIG. 12. Number of CH_4 molecules produced during the K_2CO_3- and KOH-catalyzed water–graphite reactions as a function of reaction time for two different temperatures. For the KOH-catalyzed reaction, only the steady-state production of CH_4 is plotted.

In order to ascertain that the CH_4 production from KOH–graphite was catalytic, the production of CH_4 at 522 K was measured for a period of 20 hr and is plotted in Fig. 11. The rate of CH_4 evolution stays constant at turnovers greater than 10 molecules per site. In order to scale up methane production by using higher surface area samples, graphite powder impregnated with KOH was placed in a quartz reactor and a mixture of water and helium was introduced at a flow rate of 30 ml/min. The temperature of the oven was raised to 522 K and after a period of 1 min methane was readily detected.

The behavior of methane production in this flow reactor was the same as previously observed with the high-pressure–low-pressure system; a burst of methane was detected during the first 10 min of reaction time, then the CH_4 production rate slowed down and reached a steady state. Whenever the graphite powder was impregnated with fresh KOH, a new burst of CH_4 was detected. This behavior can either be explained by the reduction of the contact surface between the graphite and the KOH, or by KOH undergoing a chemical transformation into a potassium compound which is less active in catalyzing this reaction.

The K_2CO_3–Graphite System

This system was studied in detail at only two temperatures, 495 and 522 K, since it behaves similarly to the potassium–graphite systems previously investigated. The CH_4 production at these two temperatures is plotted as a function of time in Fig. 12. In this same figure we have plotted the steady-state production of CH_4 from the KOH–graphite system at the same temperatures.

The KOH–graphite and K_2CO_3–graphite behave identically in the steady-state production of CH_4 as indicated in this figure. The CO_2 and CO concentrations are plotted in Figs. 13 and 14, respectively. Much more CO_2 is produced because the water–gas shift reaction is better catalyzed by K_2CO_3–graphite than by the KOH–graphite system at the same temperature (see Fig. 13). We have also plotted in this figure the CO_2 produced at 495 K in a blank experiment (when graphite is replaced by a gold foil coated with K_2CO_3) as represented by open hexa-

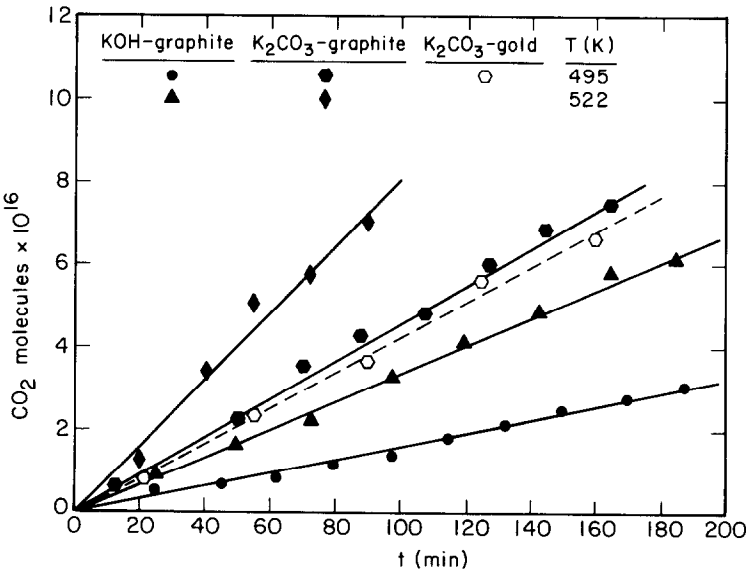

FIG. 13. Number of CO_2 molecules produced during the K_2CO_3- and KOH-catalyzed water–graphite reactions as a function of reaction time for two different temperatures. Open hexagons correspond to a blank experiment performed with K_2CO_3-covered gold foil at 495 K.

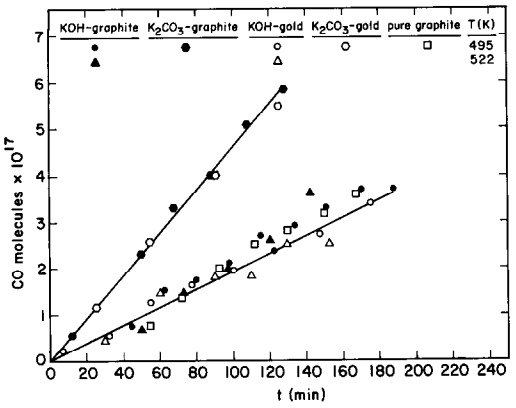

FIG. 14. Number of CO molecules produced during the K_2CO_3- and KOH-catalyzed water–graphite reactions as a function of reaction time for two different temperatures. Open hexagons, open triangles, and open circles correspond to blank experiments performed with K_2CO_3- and KOH-covered gold foils at various temperatures. Open squares correspond to pure graphite at 495 K.

gons. It seems that at low temperatures, the mechanism responsible for the CH_4 production can be described once more by the reaction represented by Eq. (1). The CO buildup in the gas phase is now higher than in the previous cases; nevertheless, blank experiments performed with gold foils coated with K_2CO_3 indicate that this extra CO in the gas phase is not a result of the decomposition of K_2CO_3.

The LiOH–, NaOH–, and CsOH–Graphite Systems

Different samples of graphite coated by impregnation with 0.38 *M* solutions of LiOH, NaOH, and CsOH were studied as potential methanation catalysts and compared with the KOH–graphite system. These samples were studied at 522 K and all of the alkali hydroxides proved to be good catalysts for the production of methane from water and graphite. The experimental conditions were identical to those used for the K, KOH, K_2CO_3–graphite systems. The CH_4 concentration at 522 K is plotted as a function of time in Fig. 15. One can see that KOH–, CsOH–, and NaOH–graphite yielded nearly the same CH_4 production rates in the steady state, but LiOH–graphite is clearly more active. On the other hand, the initial rate of CH_4 production follows the sequence CsOH, KOH, NaOH, and LiOH from the highest to the lowest initial rate. Once the rate of methanation is calculated per carbon site, the turnover frequency obtained for LiOH–graphite is almost 2.5 times higher than CsOH–graphite and KOH–graphite, and about 4 times higher than NaOH–graphite (Table 1). It should be noted that the activity of these hydroxides for CH_4 production at low temperatures follows the same correlation as the activity of the corresponding carbonates for graphite gasification at high temperatures as studied by McKee and Chatterji (*9*). These samples were also inspected by scanning electron microscopy, and crystallite formation containing the alkali metals were found in all cases after the samples were exposed to reaction conditions (after the steady-state production of CH_4 was reached). The largest crystallites were found in the case of CsOH with an average size of ~30 μm; for NaOH and LiOH ~4 μm. The ratio between the initial and the steady-state rate of CH_4 production

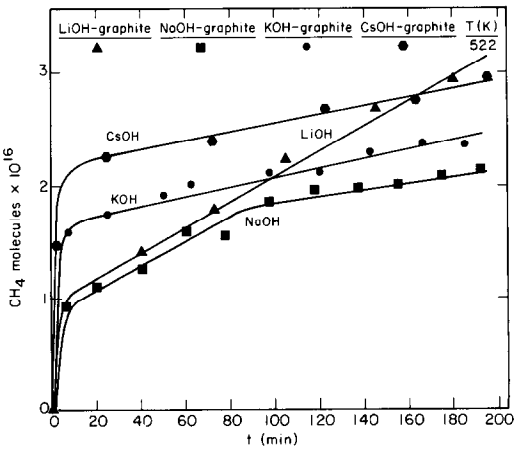

FIG. 15. Number of CH_4 molecules produced during the LiOH-, NaOH-, KOH-, and CsOH-catalyzed water–graphite reactions as a function of reaction time at 522 K.

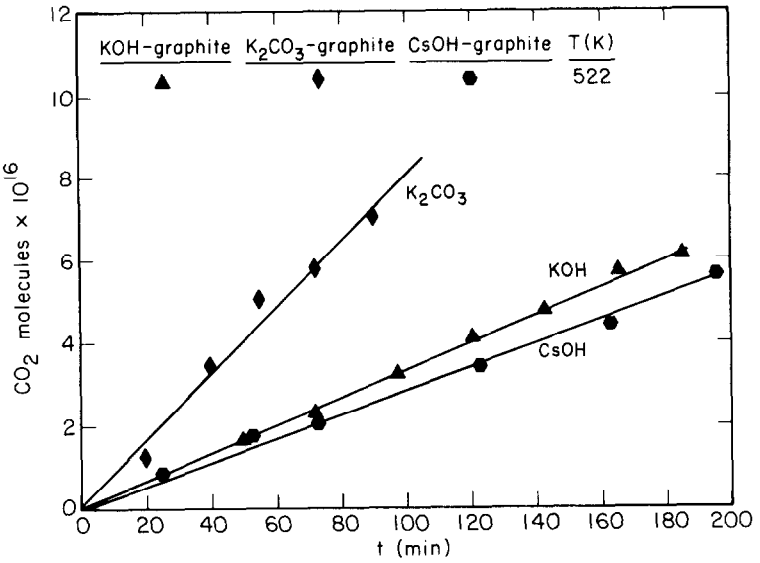

FIG. 16. Number of CO_2 molecules produced during the K_2CO_3-, KOH-, and CsOH-catalyzed water–graphite reactions as a function of time at 522 K.

correlates well with the size of the crystallites formed for the different alkali hydroxides. This reduction in contact area between the catalyst and the graphite might account in part for the reduction of the rate of CH_4 production after the first few minutes of the reaction (see Fig. 15). It is likely that the rate during steady-state production of CH_4 might be closely related to the state of dispersion of the different hydroxide catalysts.

The CO_2 and CO concentrations obtained in these experiments are displayed in Figs. 16 and 17, respectively. In the LiOH–graphite and NaOH–graphite systems no CO_2 was produced, indicating that CH_4 formation occurs according to Eq. (3). No attempt was made in this case to measure the CO or CO_2 buildup in a blank experiment.

Thermal Desorption Experiments

Thermal desorption experiments were performed over a piece of gold foil coated with KOH in order to study the thermal stability of this hydroxide. The base pressure of the system was $<10^{-9}$ Torr before the gold was resistively heated up to 1200 K at a rate of 10 K/sec. The hydrogen, oxygen, and potassium peaks were scanned with the mass spectrometer during heating. The evolution of H_2 was detected around 400 K and potassium (mass 39) was detected at a higher temperature, 775 K, as shown in Fig. 18, but no O_2 (mass 32) was detected until the temperature of ~990 K was reached. The desorption of metallic potassium from graphite takes place at about the same temperature as from gold. Since KOH is very stable toward dissociation (*10*), hydrogen evolution at 400 K might come from the dissociation of chemisorbed water over this system. The potassium peak is detected near the temperature range at which KOH vaporized. The high flux of K^+ ions is a result of KOH cracking due to ionization (*10*).

H_2 Desorption

One of the intermediate steps in the production of CH_4 is the formation of CH_x complexes on the surface of the graphite. If one interrupts the production of CH_4 from the alkali hydroxide–graphite systems, the surface of the samples should have adsorbed CH_x complexes which, upon heating, will decompose to yield molecular hy-

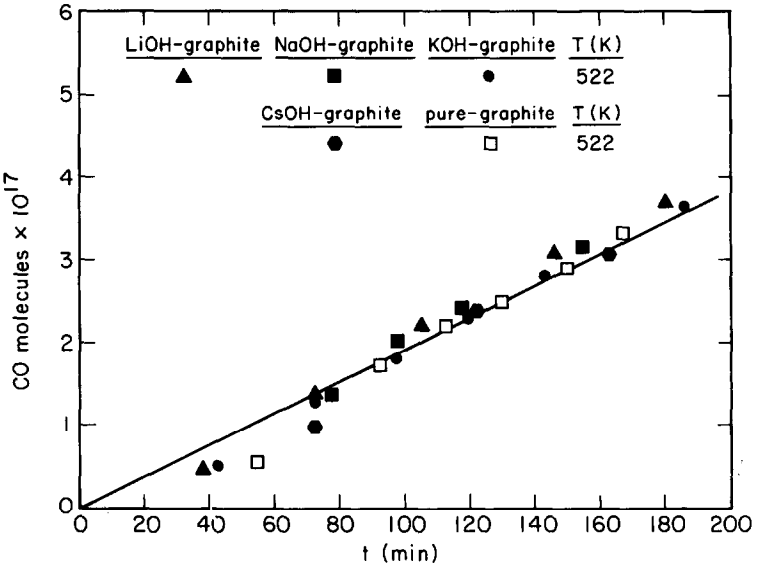

FIG. 17. Number of CO molecules produced during the LiOH-, NaOH-, KOH-, and CsOH-catalyzed water–graphite reactions as a function of reaction time at 522 K. Open squares correspond to pure graphite at the same temperature.

drogen (desorbing to the gas phase) and leaves carbon atoms on the surface. This decomposition must take place at high temperatures because of the formation of strong bonds by carbon and hydrogen atoms. Salmeron and Somorjai (*11*) studied the decomposition of unsaturated hydrocarbons on the Pt(111) crystal face and they found that the complete dehydrogenation of these hydrocarbon fragments took place between 550 and 710 K. Therefore, each of the systems studied in the CH_4 production was flashed to 1200 K, after the reaction with water. A strong hydrogen peak was detected at high temperatures. Thermal desorption spectra of hydrogen desorption from LiOH–, NaOH–, KOH–, and CsOH–graphite are displayed in Fig. 19.

In order to make sure that the H_2 was not hydrogen from the alkali hydroxide com-

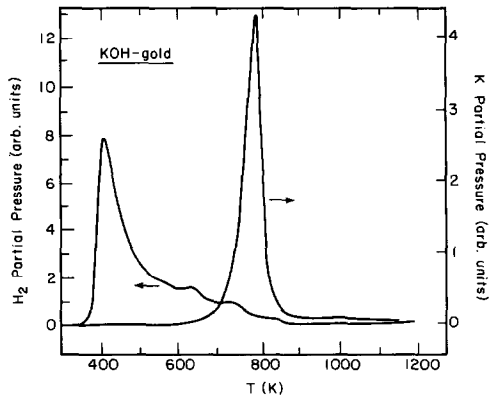

FIG. 18. Thermal desorption of H_2 and K from a KOH-covered gold foil sample.

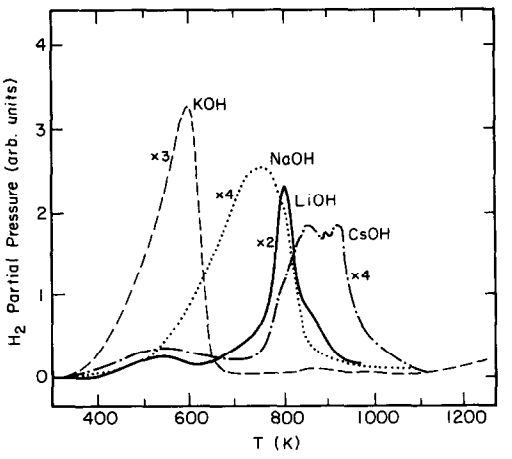

FIG. 19. Thermal desorption of H_2 from LiOH–, NaOH–, and KOH–, and CsOH–graphite samples after exposure to reaction conditions.

pounds, a piece of gold foil was coated with the different alkali hydroxides and flashed in ultrahigh vacuum up to 1200 K. H_2 was detected at much lower temperatures in each case and these desorption spectra are also displayed in Fig. 20. Although we cannot ascertain the amount of H_2 that is produced from the CH_x complexes decomposition due to the high H_2 background, the shift of the H_2 peaks to higher temperatures (after CH_4 is produced) is a strong indication of the presence of these complexes on the graphite surface. The temperature at which the H_2 peak is observed is a measure of the C–H bond strength. It should be noted that the amount of H_2 released from this decomposition is of order of monolayers.

The formation of CH_4 from graphite and H_2O is a process of considerable complexity that requires many sequential reaction steps. The catalysts (alkali hydroxides) must aid in the dissociation of H_2O on the graphite surface and possibly in the breaking of C–C bonds in the graphite previous to the formation of the CH_4 molecule. The OH^- and H^+ produced from H_2O dissociation then participate in the multiple step oxidizing and reducing reactions. It is known that atomic hydrogen forms C–H bonds with graphite that leads to the production of CH_4 molecules at low temperatures (400–800 K) (*8*). On the other hand, the OH^- must somehow donate its oxygen to produce C–O bonds and eventually desorbed CO or CO_2. The use of high-density oxygen-free graphite rules out the possibility that oxygen and hydrogen in the final gaseous products, CH_4 and CO or CO_2, could come from sources other than the water molecules.

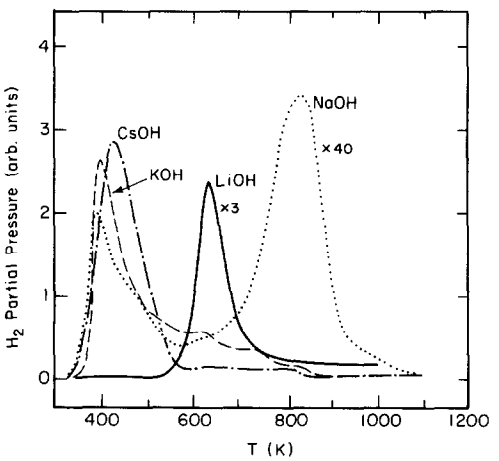

FIG. 20. Thermal desorption of H_2 from LiOH-, NaOH-, KOH-, and CsOH-covered gold foil samples.

Further studies aimed at exploring the mechanism of this catalyzed reaction include attempts to detect CH_x and COH intermediates by electron spectroscopy and exploration of the possibility of K intercalation into the graphite that may be an important reaction step needed to break the C–C bonds of the reactant efficiently. The use of alkaline earth compounds as possible catalysts will be investigated to optimize the activity of the carbon–water (C/H_2O) reaction. The combination of transition metals and alkali–metal compounds as catalysts should be explored in order to aid the formation of gaseous hydrocarbon molecules other than CH_4.

CONCLUSIONS

The production of gaseous CH_4 and CO_2 (or CH_4 and CO) from graphite occurs rapidly in the temperature range 500–650 K with low activation energy (10 ± 3 kcal) in the presence of alkali compounds. KOH, K_2CO_3, LiOH, CsOH, and NaOH all appear to catalyze both the reduction of C to CH_4 and its oxidation to CO_2 or CO.

Using high surface area graphite, we have shown that scaling up the C/H_2O reaction to produce large amounts of CH_4 gas can readily be accomplished. Thus this reaction can be carried out under technologically feasible conditions. One should then consider other, more economical sources of carbon to produce CH_4, such as coal, biomass, including wood or other plant sources.

ACKNOWLEDGMENTS

This work was jointly supported by the Director,

Office of Energy Research, Office of Basic Energy Sciences, Chemical Sciences Division, and the Assistant Secretary for Fossil Energy, under Contract Number W-7405-ENG-48, through the Pittsburgh Energy Technology Center, Pittsburgh, PA.

REFERENCES

1. Wen-Yang Wen, *Catal. Rev. Sci. Eng.* **22,** 1 (1980).
2. US Patent 4,094,650, Koh *et al.*, Exxon Research and Engineering Co., June 13, 1978.
3. Blakely, D. W., Kozak, E. I., Sexton, B. A., and Somorjai, G. A., *J. Vac. Sci. Technol.* **13,** 1091 (1976).
4. Marbrow, R. A., and Lambert, R. M., *Surface Sci.* **6,** 329 (1976).
5. Rhead, G. E., *J. Vac. Sci. Technol.* **13,** 603 (1976).
6. Kokes, R. J., Tobin, H., and Emmett, P. H., *J. Amer. Chem. Soc.* **77,** 5860 (1955).
7. Luengo, C. A., Cabrera, A. L., MacKay, H. B., and Maple, M. B., *J. Catal.* **47,** 1 (1977).
8. Balooch, M., and Olander, D. R., *J. Chem. Phys.* **63,** 4772 (1975).
9. McKee, D. W., and Chatterji, D., *Carbon* **13,** 381 (1975).
10. Porter, R. J., and Schoonmaker, R. C., *J. Phys. Chem.* **62,** 234 (1958).
11. Salmeron, M., and Somorjai, G. A., *J. Phys. Chem.*, in press.